Dissolved organic matter and heterotrophic prokaryotes diel patterns reveal enhanced growth at the mesopelagic fish layer during daytime

Xosé Anxelu G. Morán[1*], Francisca C. García[1,2], Anders Røstad[1], Luis Silva[1], Najwa Al-Otaibi[1], Xabier Irigoien[3], Maria L. Calleja[1, 4]

[1]King Abdullah University of Science and Technology (KAUST), Red Sea Research Center, Biological and Environmental Science & Engineering Division, 23955-6900 Thuwal, Saudi Arabia

[2]Environment and Sustainability Institute, University of Exeter, TR10 9FE Penryn, United Kingdom

[3]AZTI Tecnalia, 20110 Pasaia, Spain

[4]Max Planck Institute for Chemistry, 55128 Mainz, Germany

*Corresponding Author. Phone: +966 (0)128082455. Email: xelu.moran@kaust.edu.sa

ABSTRACT

Contrary to epipelagic waters, where biogeochemical processes closely follow the light and dark periods, little is known about diel cycles in the mesopelagic realm. Here, we monitored the dynamics of dissolved organic matter (DOM) and planktonic heterotrophic prokaryotes every 2 h for one day at the surface and 550 m (a depth occupied by mesopelagic fish during light hours) in oligotrophic waters of the central Red Sea. We additionally performed predator-free seawater incubations of samples collected from the same site at midnight and noon. Comparable variability in microbial biomass and dissolved organic carbon in situ suggests a diel supply of fresh DOM in both layers. The presence of mesopelagic fishes during daytime promoted a sustained, longer growth of larger prokaryotic cells, with specific growth rates consistently higher in both noon experiments (surface: 0.34 vs. 0.18 d^{-1}, deep: 0.16 vs. 0.09 d^{-1}). Heterotrophic prokaryotes in the mesopelagic fish layer were also more efficient at converting DOM into new biomass. These results suggest that the ocean's twilight zone receives a continuous diurnal supply of labile DOM from diel vertical migrating fishes, enabling an unexpectedly active community of heterotrophic prokaryotes.

Keywords: diel cycles, heterotrophic prokaryotes, mesopelagic fishes, vertical migration, carbon fluxes.

INTRODUCTION

Planktonic heterotrophic prokaryotes (HP) pertaining to the domains Bacteria and Archaea rely on labile dissolved organic matter (DOM) for metabolism and growth (Carlson et al. 1994, Goldman and Dennett 2000, Pomeroy et al. 2007). In surface waters, diel cycles in HP biomass and activity have been related to the photosynthetic activity of phytoplankton (Gasol et al. 1998), which obviously follows sunlight. Heterotrophic prokaryotes dependence of DOM derived from planktonic algae (Baines and Pace 1991) was reported to increase offshore, as we moved away from coastal inputs, in temperate and polar ecosystems (Morán et al. 2001). Although this relationship also known as bacterioplankton-phytoplankton coupling was questioned (Fouilland and Mostajir 2010), but see (Morán and Alonso-Sáez 2011), in regions with low DOM advection (e.g. at permanently stratified sites without anthropogenic or riverine inputs nearby, such as oligotrophic tropical waters), we might expect strong diel signals in the response of heterotrophic prokaryotes coupled with the activity of primary producers (Ruiz-González et al. 2012). In this regard, the Red Sea offers a unique opportunity to study biogeochemical processes in oligotrophic ecosystems. With no permanent rivers, the only allochthonous inputs of DOM come from urban centers such as Suez, Ghardaqa, Jeddah or Port Sudan, coastal macrophytes (Alongi and Mukhopadhyay 2015, Duarte and Cebrián 1996) or dust events (Bao et al. 2018, Lekunberri et al. 2010).

While epipelagic processes driven by primary production are well known (Henson et al. 2012, Herndl and Reinthaler 2013), large gaps in our understanding of the ecology and biogeochemistry of the mesopelagic zone (i.e. waters between 200 m and 1000 m) remain (Robinson et al. 2010). In the mesopelagic realm, trophic interactions between microbes and metazoa have been long neglected. The available studies have focused mostly on mesozooplankton (e.g., (Al-Mutairi and Landry 2001, Bianchi et al. 2013, Isla et al. 2015). However, recent reports on the large biomass contributed to the ocean's biota by mesopelagic fishes performing diel vertical migration (DVM, (Irigoien et al. 2014, Klevjer et al. 2016) suggest they may also play an important role as rapid vectors of labile organic mater. DVM can affect only a fraction or the entire community (Klevjer et al. 2016). In the Red Sea, the entire populations of mesopelagic fishes migrate daily between the surface and the so-called deep

scattering layer (DSL) located at 400-650 m in the mesopelagic zone (Klevjer et al. 2012, Røstad et al. 2016). DVM fishes have been recently suggested to generate hotspots for heterotrophic prokaryotes, yielding significantly higher bacterial growth efficiencies compared with shallower layers (Calleja et al. 2018). An analysis of a 24 h intensive sampling at the same location has supported the existence of diel inputs of labile DOM fueling the HP community at the depths occupied by mesopelagic fishes during daytime (García et al. 2018). Both DOC concentrations and the contribution of high nucleic acid content (HNA) bacteria, usually made up of copiotrophic taxa (Schattenhofer et al. 2011, Vila-Costa et al. 2012) more active than the low nucleic acid content (LNA) group (e.g. (Bouvier et al. 2007, Gasol et al. 1999, Morán et al. 2011), fluctuated as widely in waters below 200 m as in the upper layers. However, for the hypothesis of the mesopelagic labile DOM hotspots to be true, we should be able to demonstrate that the presence or absence of fishes in the twilight zone does make a difference.

Here, we report on the results of two short-term incubations with water collected from the epi- and mesopelagic layers (surface and 550 m, respectively) of the central Red Sea at midnight and at the following midday. After removing protistan grazers and other larger organisms by filtration, we followed the dynamics of DOM-heterotrophic prokaryotes interactions for 8 days. In parallel, we conducted a high frequency (every 2 h for a full 24 h starting at noon) characterization of the same depths focusing on the response of heterotrophic prokaryotes abundance, cell size and biomass to changes in DOM concentrations including its fluorescent properties, previously unreported for this basin. The specific objectives of this study were: i) to assess the diurnal scales of variability in the standing stocks of HP and DOM in epipelagic and mesopelagic waters of the central Red Sea, and ii) to test for differences in the specific growth rate, maximum biomass and growth efficiency of HP between nighttime and daytime in both layers. Our hypothesis is that DOM supplied by DVM fishes in the mesopelagic zone during the day had a commesurable effect on the above-mentioned variables.

MATERIALS AND METHODS

Environmental sampling

We occupied one station located 13.4 km offshore to the north of King Abdullah Economic City, Saudi Arabia (lat 22.46°N, lon 39.02°E) between noons of March 6th and 7th 2016 (Calleja et al. 2018, García et al. 2018). Sampling was conducted on board of RV Thuwal. Continuous acoustic measurements in order to locate the position of the vertically migrating mesopelagic fishes were recorded with a Simrad EK60 38 kHz echosounder mounted on the ship's hull. From noon on March 6th until the same time on the following day we conducted CTD casts every 2 hours. At each cast we sampled discrete depths in the water column with Niskin bottles mounted on a Rosette sampler, ranging from the surface to 650 m depth. Water filtered through pre-combusted Whatman GF/F filters was collected for analyzing DOC bulk concentrations and fluorescent DOM (FDOM) properties (40 mL pre-combusted glass vials). Unfiltered water was collected for characterizing the community of heterotrophic prokaryotes (2 mL cryovials).

Hourly apparent DOC production and consumption rates were estimated as the largest difference between DOC concentration in consecutive sampling times consistently increasing and decreasing, respectively. The same approach was used for estimating the apparent biomass production of heterotrophic prokaryotes over the diel cycle.

Experimental incubations

10 L of seawater from the surface and 550 m depth were collected in the midnight and noon casts on March 7th for conducting the experimental incubations of DOC consumption, change in FDOM and heterotrophic prokaryotes biomass response. In order of remove protistan grazers and planktonic organisms larger than bacteria and archaea, water was gently filtered through pre-combusted Whatman GF/C filters (142 mm, nominal pore size 1.2 µm) and used to fill 3 x 2 L acid-cleaned polycarbonate bottles, which were subsequently incubated at in situ temperature and light regime (darkness for 550 m samples). Removal of prokaryotic cells by filtration was minor (83% ± 7% SE of the initial abundance was retrieved in the water used for the incubations) and mean cell size was virtually unaffected (2.6% ± 1.0% smaller biovolume than inthe unfiltered water). Filtration virtually eliminated all protistan grazers of heterotrophic

prokaryotes, since the mean abundance of heterotrophic nanoflagellates in the GF/C filtrate was 1.5% (E. I. Sabbagh, pers. comm.) Subsamples were taken twice per day on the first 2 days, then daily until day 6 and finally at day 8. DOC and FDOM subsamples from the incubations were filtered through 0.2 Millipore polycarbonate filters. We will occasionally use the codes S and F to refer to the incubations made with water from the Surface (0 m) and the Fish layer (550 m), respectively, followed by D or N to refer to the period of sampling (Day or Night): SD, SN, FD, FN.

DOC analysis

Samples for DOC were acidified with H_3PO_4 and kept in the dark at 4 °C until analysis by high temperature catalytic oxidation at the laboratory. All glass material used was acid cleaned and burned (450°C, 4.5 h). Consensus reference material of deep sea carbon (42–45 µmol C L^{-1} and 31-33 µmol N L^{-1}) and low carbon water (1-2 µmol C L^{-1}), provided by D. A. Hansell and W. Chen (Univ. of Miami) was used to monitor the accuracy of our DOC concentration measurements. The analytical error of DOC concentration was 1.4 µmol L^{-1}.

DOM fluorescence measurements and PARAFAC modeling

UV-VIS fluorescence spectroscopy was measured using a HORIBA Jobin Yvon AquaLog spectrofluorometer with a 1 cm path length quartz cuvette. Three dimensional fluorescence excitation emission matrices (EEMs) were recorded by scanning with an excitation wavelength range of 240- 600 nm and emission of 250-600 nm, both at 3 nm increments and integrating at 8 seconds. To correct and calibrate the fluorescence spectra post-processing steps were followed according to Murphy et al. (Murphy et al. 2010). Briefly, fluorescence spectra were Raman area (RA) normalized by subtracting daily blanks that were performed using Ultra-Pure Milli-Q sealed water (Certified Reference, Starna Cells). Inner-filter correction (IFC) was also applied according to McKnight et al. (2001) RA normalization, blank subtraction, IFC and generation of EEMs were performed using MATLAB (version R2015b).

A total of 165 samples for DOM fluorescence were collected (81 from 7 vertical profiles and 84 from the experimental incubations). The EEMs obtained were subjected to PARAFAC

156 modeling using DOMFluor Toolbox (Stedmon and Bro 2008). Before the analysis, Rayleigh
157 scatter bands were trimmed. A four-component model was validated using split-half validation
158 and random initialization (Stedmon and Bro 2008): peak C1 at Ex/Em 240(325)/ 407 nm, peak
159 C2 at Ex/Em 258(390)/492 nm, peak C3 at Ex/Em 240/337 and peak C4 at Ex/Em 276/312 nm.
160 C1 corresponds to peak M (Coble 2007) and is comparable to component 2 identified by Català
161 et al. (Catalá et al. 2015). C2 represents a combination of peaks A and C (Coble 2007) and is
162 comparable to component 1 in (Catalá et al. 2015). C3 corresponds to peak T (Coble 2007),
163 attributed to tryptophane, and is comparable to component 3 in (Catalá et al. 2015). C4
164 corresponds to peak B (Coble 2007), attributed to tyrosine, and is comparable to component 4
165 in (Catalá et al. 2015). The maximum fluorescence (Fmax) is reported in Raman units (RU).
166
167 **Heterotrophic prokaryotes abundance and biomass**
168 Triplicate samples (1.8 mL) for estimating the abundance of heterotrophic bacteria and
169 archaea in situ and in the experimental incubations were fixed with 1% paraformaldehyde and
170 0.05% glutaraldehyde, deep frozen in liquid nitrogen and stored at -80°C until analysis. Once
171 thawed, 400 µL aliquots were stained with SYBR-Green run in a BD FACSCanto II flow cytometer
172 for estimating the abundance of low (LNA) and high (HNA) nucleic acid content cells as detailed
173 in Gasol and Morán (Gasol and Morán 2015). The Abundances were estimated based on time
174 and the actual flow rates, which were calibrated daily using the gravimetric method. The right
175 angle light scatter or side scatter (SSC) signal relative to the value of 1 µm fluorescent latex
176 beads added to each sample was used to estimate the cell diameter according to Calvo-Díaz
177 and Morán (Calvo-Díaz and Morán 2006). LNA and HNA cell numbers were summed to estimate
178 the total abundance and their specific cell sizes averaged to obtain the mean cell size of the
179 heterotrophic prokaryote community at both depths and different times. Assuming spherical
180 shape, the mean cell size (biovolume in μm^3) was converted into cellular carbon content
181 following Gundersen et al. (Gundersen et al. 2001). Heterotrophic prokaryotes biomass was
182 then calculated as the product of cell abundance and mean cellular carbon content.
183
184 **Growth rate estimates**

In situ apparent or net growth rates of the heterotrophic prokaryote assemblage at the surface and the mesopelagic fish layer were estimated from changes in biomass (µg C L^{-1}) resulting from changes in abundance and mean cell size over 24 h. Net growth rates (µ, in units h^{-1}) were calculated as:

$$\mu = \ln (N_1/N_0) / \Delta t \quad (1)$$

where N_1 is the final biomass, N_0 is the initial biomass and Δt is the time interval (2 h). We modeled the overall daily growth rate from Eq. (1) using the size distribution of the organisms with the R package ssPopModel, which included a modified version of the size-structured matrix population model originally developed by Sosik et al. (Sosik et al. 2003). Matrix population model assumption is that changes in size distribution are only related to growth and division of the cells. We adapted and simplified the application of this function as described by Hunter-Cevera et al. (Hunter-Cevera et al. 2014) for *Synechococcus* cyanobacteria to be used with heterotrophic prokaryote cells.

Specific growth rates in the incubations were calculated as the slope of the ln-transformed total abundance vs. time for the linear response period, equivalent to the phase of exponential growth (usually lasting between 2 and 3 days).

Prokaryotic growth efficiency

Prokaryote heterotrophic production (PHP) in the midnight and midday incubations was estimated as the rate of increase in bacterial biomass during the exponential phase of growth. Prokaryotic carbon demand (PCD, i.e. the sum of heterotrophic prokaryotes production and respiration) was approached by the consumption rate of DOC during the same period. Prokaryotic growth efficiency (PGE) was therefore calculated as the ratio of PHP to PCD.

Statistical analyses

Model I or ordinary least squares (OLS) linear regressions for estimating specific growth rates were done separately for each replicate, using a common period for each experiment.

Differences between treatments and/or depths were assessed with one way ANOVAs and Fisher least significance (LSD) post-hoc tests. General relationships between variables were represented by Pearson's correlation coefficients. Statistical analyses were done with JMP and STATISTICA software packages.

RESULTS

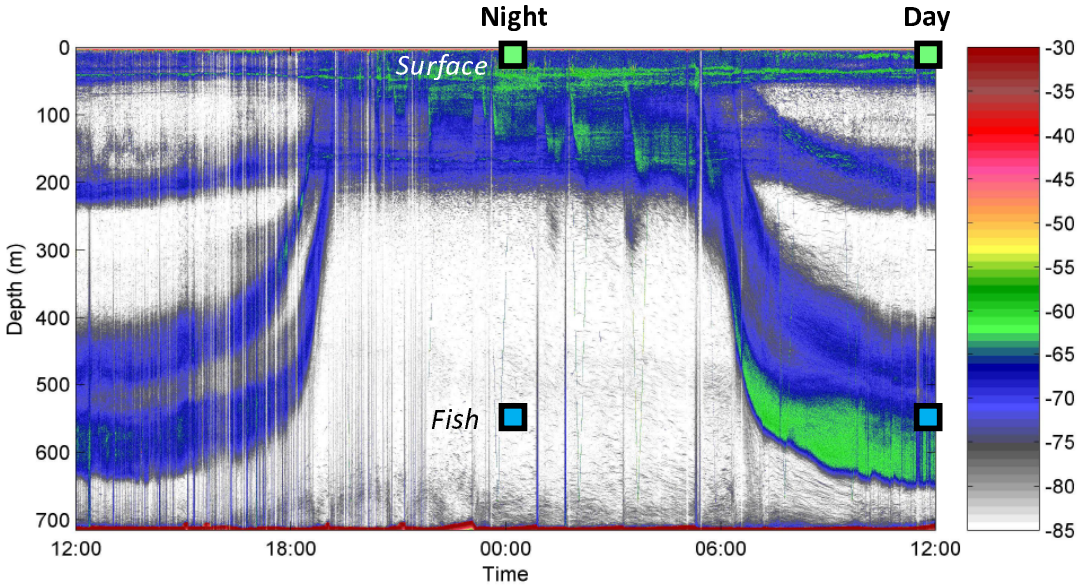

Fig. 1. Echogram from March 5th to 6th 2016 at the study site showing 2 scattering layers of mesopelagic fish performing diel vertical migration: up to the surface at night and down to deep waters during daytime. Symbols indicate the depth and time of water collection for the incubation experiments.

Environmental variability of DOC and heterotrophic prokaryotes

The complete diel vertical migration of the mesopelagic fishes present at the study site can be clearly seen in the echogram of **Fig. 1**, with the deeper, more intense layer (dominated by *Benthosema pterotum*) occupying the depths between ca. 520 and 630 m during daytime on March 6th 2016. **Fig. 2** shows the diel variability of DOC concentrations and the biomass of HP at the station's surface and 550 m depth. Mean DOC values were almost 50% higher at 0 than at 550 m (71.0 ± 1.6 SE and 45.6 ± 1.5 µmol C L^{-1}, respectively). Both depths showed similar dynamics, with two relative maximaof DOC at around midnight and noon (**Fig. 2A**). The

midnight peak was higher and more conspicuous at the surface than at the fish layer. However, both depths displayed a similar diel variability with slightly higher CV in the fish layer (8.1% vs. 5.7%). From these values we were able to estimate apparent production and consumption rates. The hourly rates of DOC production (from 8 am to 12 pm) and consumption (from 12 am to 8 am at the surface and from 12 pm to 4 pm at 550 m) were similar within each layer: ca. 1.3 µmol C L^{-1} h^{-1} at the surface and 2.0 µmol C L^{-1} h^{-1} at the fish layer. The protein (Tyrosine)-like fluorescent DOM component C4 was on average one order of magnitude higher at the surface than at 550 m, although it showed more variability at depth (**Table S1**).

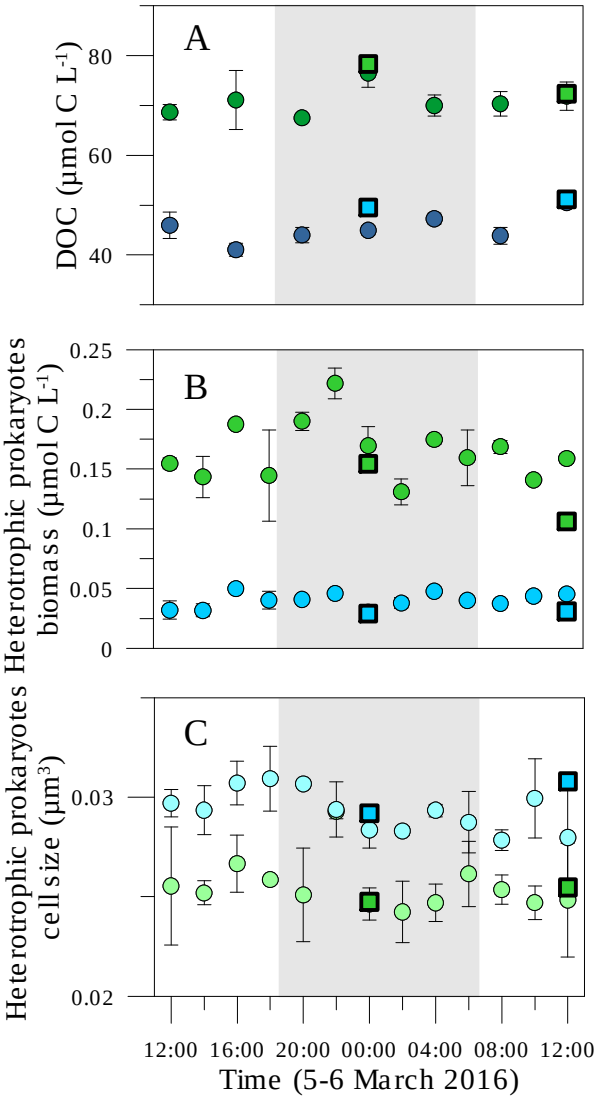

Fig. 2. Variability of mean DOC concentration (**A**) and heterotrophic prokaryoplankton biomass (**B**) and cell size (**C**) in two layers of the study site: upper (0-25 m) and mesopelagic occupied by fish during daytime (450-600 m) during the 24 h sampling. Squares indicate initial values at the onset of the experimental incubations. The gray

area represents nightime hours at the date of sampling. Error bars represent the standard error of the mean (average of 0 and 25 m in the upper layer and 450, 550 and 600 m in the mesopelagic one).

The abundance of HP at the surface (mean 4.31 ± 0.17 x 10^5 cells mL^{-1}) was also one order of magnitude higher than at 550 m (mean 9.43 ± 0.39 x 10^4 cells mL^{-1}), but varied similarly with no clear diel patterns. Although their size was 22% ± 8% larger in the mesopelagic (mean values of 0.034 and 0.028 μm^3 at the fish and surface layers, respectively, **Fig. 2C**), the corresponding biomass was driven mostly by changes in abundance, averaging 1.91 ± 0.09 µg C L^{-1} at the surface and 0.50 ± 0.02 µg C L^{-1} at 550 m. **Fig. 2B** (in µmol C L^{-1} for comparison with **Fig. 2C**) shows that HP biomass was equally variable at both layers (CV 16.0 vs. 16.3%). In situ apparent or net growth rates based on changes in HP cell size were of 0.15 and 0.10 d^{-1} at 0 and 550 m, respectively. HP cell specific growth rates changed cyclically over the 24 h cycle in both depths (**Fig. S2**). Two maxima, at 20:00 and 8:00, were found at the surface layer while the maximum at 550 m was observed at 16:00

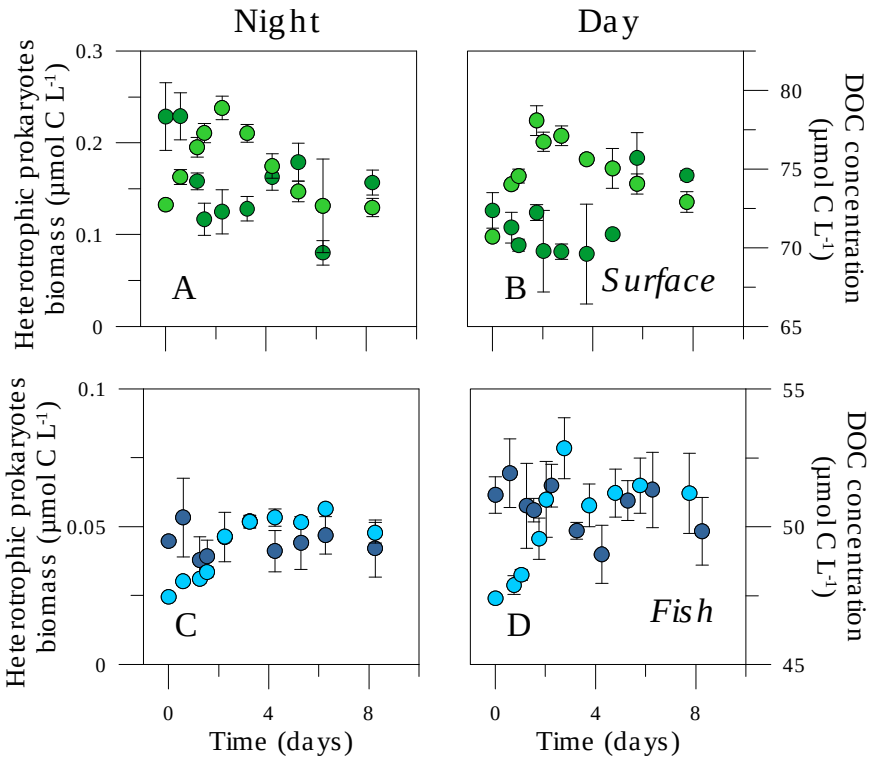

Fig. 3. Dynamics of heterotrophic prokaryoplankton biomass and DOC concentration in the predator-free experimental incubations of samples taken at noon (**A, C**) and at midnight (**B, D**) from the surface and 550 m depth. Error bars are standard errors of 3 replicates.

Table 1. Mean ± SE values of specific growth rates (μ), DOC consumption rates or prokaryotic carbon demand (PCD, see the text), prokaryotic heterotrophic production rates (PHP) and prokaryotic growth efficiency (PGE) in the surface and fish layer incubation experiments performed at noon (Day) and midnight (Night). Rates were calculated for each period of exponential growth, also indicated in days. The same period was used for DOC consumption and biomass production rates. Also indicated are the maximum heterotrophic prokaryotes biomass reached within the incubation and the corresponding ratio of maximum to initial biomass (Max:t0 biomass ratio).

Layer	Time	Period (d)	μ (d^{-1})	DOC consumption rate (μmol C L^{-1} d^{-1})	PHP rate (μmol C L^{-1} d^{-1})	PGE (%)	Maximum HP biomass (μg C L^{-1})	Max:t0 HP biomass ratio
Surface	Day	0-1.75	0.34 ± 0.07	1.0 ± 0.5	0.040 ± 0.004	4.2	2.69 ± 0.20	2.30
	Night	0-2.25	0.18 ± 0.02	2.7 ± 1.1	0.047 ± 0.006	1.8	2.85 ± 0.16	1.80
Fish	Day	0-2.75	0.16 ± 0.04	0.5 ± 0.3	0.020 ± 0.004	4.2	0.94 ± 0.13	3.27
	Night	0-2.25	0.09 ± 0.01	0.3 ± 0.8	0.010 ± 0.001	3.1	0.68 ± 0.02	2.31

Experimental incubations of surface and deep samples

With initial concentrations similar to ambient values (**Fig. 2**), DOC was consumed in the first 2-3 days in the predator-free experiments (**Fig. 3**), albeit at different daily rates (**Table 1**), followed by net production after day 4 especially in the Surface incubations. Minimum and maximum consumption rates were 0.32 and 2.69 μmol C L^{-1} d^{-1}, found in the Fish and Surface Night experiments, respectively (FN and SN). Values in the other two experiments carried out with noon samples were below 1 μmol C L^{-1} d^{-1} (0.47 and 0.95 μmol C L^{-1} d^{-1}, respectively in in FS and SD). The initial fluorescence intensity values of the component C4 in the experiments was higher but reflected the values measured concurrently in the water column (paired *t*-test, $p>0.05$, $n=4$). C4 showed a very consistent consumption pattern regardless of the layer and treatment. Heterotrophic prokaryotes in the Surface incubations consumed in 4 days 40 and 50% of the initial values during Night and Day respectively, while bacteria inhabiting deep waters consumed almost all of it (95-100 %) within the same time frame regardless of the

sampling time (**Fig. 4**). Hereinafter we consider changes in C4 as representative of labile DOM dynamics. Day and night C4 consumption patterns did not show any significant differences within the same layer but they displayed significantly higher consumption rates in the Fish layer (ANOVA, p=0.004, post-hoc Fisher LSD test, **Figure 4** and **Table S1**).

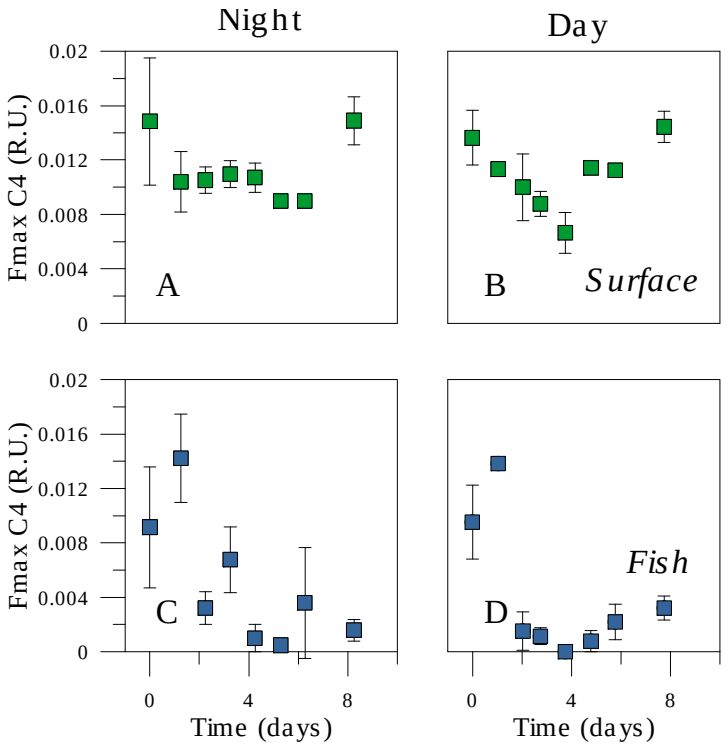

Fig. 4. Dynamics of the concentration of the FDOM protein-like C4 component in the predator-free experimental incubations of samples taken at noon (**A, C**) and at midnight (**B, D**) from the surface and 550 m depth. Error bars are standard errors of 3 replicates.

Heterotrophic prokaryotes responses in the incubation experiments differed between depths and sampling times (**Fig. 3**). Consistent differences were found between the specific growth rates at both depths (**Table 1**), with μ being double in the Surface than in the Fish experiments. Within each layer, the Day μ values were also higher than the Night ones (t-tests, p=0.020 and p=0.060 at the Surface and Fish experiment, respectively, n=6). HNA cells always grew faster than their LNA counterparts resulting in increases in their relative contribution from 43-55% to 55-62%, more noticeable in the FD experiment. The mean size of the cells also increased substantially in the Fish experiments, from 0.027 to 0.060 μm^3 in the FD incubation and from 0.028 to 0.047 μm^3 in the FN one, while changes in cell size were much smaller in the

Surface experiments, and virtually the same in both periods, from 0.026 to 0.037 μm^3 (SD) and from 0.025 to 0.035 μm^3 (SN) (**Fig. S2**). Consequently, cell size played an important role in the increase in biomass, especially in both Fish experiments (**Fig. 3C, D**). The biomass production rates of heterotrophic prokaryotes for the same periods of DOC consumption ranged 4-fold, from 0.010 to 0.047 µmol C L^{-1} d^{-1}, mirroring the changes in the latter variable (**Table 1**). The rates of heterotrophic prokaryotes biomass production and DOC consumption were used for estimating prokaryotic growth efficiencies (PGE) in the four experimental incubations. PGE was uniformly below 5%, ranging from 1.8% (SN) to 4.2% (both SD and FD, **Table 1**). Following the pattern of in situ values, maximum HP biomass measured in the incubations was higher in the Surface than in the Fish experiments (**Fig. 3**, **Table 1**), although the increase ratios (i.e. the ratio of maximum to initial biomass, **Table 1**) were significantly higher in the Fish experiments with all data pooled (t-test, p=0.048 , n=12).

DISCUSSION

There is consensus that marine biota biomass and activity peak in the upper layers and decrease exponentially with depth, following the strong vertical gradients in physico-chemical properties (Arístegui et al. 2009). Heterotrophic prokaryotes inhabiting the Red Sea seem to challenge this view. Together with diel variations of standing stocks (García et al. 2018), this study), night- and day-initiated incubations of predator-free ambient assemblages with the DOM pool available at the time of sampling yielded surprising similarities in epipelagic and mesopelagic waters. A method for estimating division rates in cyanobacteria based in changes in cell size (Hunter-Cevera et al. 2014, Sosik et al. 2003) was adapted to obtain independent estimates of in situ net growth rates (**Fig. S2**). The diel variability in heterotrophic prokaryotes cell size showed the same pattern at the surface and the mesopelagic fish layer (**Fig. 2**), yielding low but comparable net growth estimates at the surface than at 550 m depth (0.10-0.15 d^{-1}). However, it must be noted here that the already large prokaryotes inhabiting the mesopelagic fish layer were able to grow much bigger in the absence of protistan grazers (**Fig. S1**), confirming the results of a previous study conducted at the same site (Calleja et al. 2018).

Diel cycles in biogeochemical properties and plankton biomass and activity in the upper ocean layers are reasonably well known, following diurnal changes in photosynthesis and food web processes (Gasol et al. 1998, Ruiz-González et al. 2012). No clear patterns were observed for in situ heterotrophic prokaryotes abundance or biomass, probably due to strong coupling between growth and mortality due to protistan grazing (Calbet et al. 2015, Silva et al.) and/or viral lysis in the Red Sea (E. Sabbagh et al., in prep.), and in tropical waters in general (Morán et al. 2017). However, likewise early observations in the Caribbean (Johnson et al. 1981) recently confirmed for this site (García et al. 2018), DOM concentrations displayed a coherent diel pattern suggesting different timing of production and consumption (**Fig. 1**). Confirming previous experiments (Calleja et al. 2018), DOC consistently decreased in the first 2-3 days in both Surface and Fish samples, ranging from 0.7 to 6.1 µmol L^{-1} , followed by net production after day 4 especially in the Surface incubations, coincident with a sharp decay in prokaryotic biomass (**Fig. 3A, B**). Indeed, the strong apparent uptake of surface DOC in situ during nighttime coincided with the highest DOC consumption experimental result, poiting to its labile nature, although the buildup of HP biomass was similar in both SD and SN experiments, resulting in lower specific growth rates and PGE values in the Night (**Table 1**). Labile DOC incorporation does not automatically inform us of its subsequent partitioning between metabolism (respiration) and growth (biomass production), as shown by Condon et al. (Condon et al. 2011) for DOM originated by jellyfish blooms. Since the alternation between light and dark periods within the incubator used for Surface seawater was common for SD and SN experiments, if photoheterotrophy (Béjà et al. 2000, Ruiz-González et al. 2013) afffected DOM dynamics, it should have been equally apparent in both Night and Day incubations, which were initiated with ony 12 h difference (**Fig. 1**). We therefore ruled out photoheterotrophic processes explaining the differences observed after 8 days of incubation. Rather, the quality of labile DOM at midday (including recent photosynthate) was probably higher than at midnight (perhaps with a greater contribution of DOM coming from sloppy feeding, (Nagata 2000), causing the significantly higher µ values (**Table 1**). That the quality of labile DOC at noon could have been higher was supported by a faster increase in bacterial cell size (**Fig. S1B**) and the contribution of HNA cells, which increased by 35% in SD compared with 15% in SN. The decrease in the protein-

like C4 component was also more sustained in the SD experiment compared to SN after 4 days (13.2% vs. 5.3% was consumed daily during that period, **Fig. 4**) although the rates were virtually the same in the initial periods (2.75 and 2.25 days, respectively, **Table S1**). Changes in mesopelagic DOC concentrations and lability at diel ((García et al. 2018), this study) and seasonal scales (Calleja et al. 2019) in the central Red Sea support the recent claim that the diverse pool of DOM in the deep ocean fluctuates at timescales much shorter than previously thought (Follett et al. 2014). Since the conditions at the study site were hypoxic in most of the mesopelagic realm (Calleja et al. 2019), the low in situ oxygen concentrations in the Fish water samples, consistent from 300 m downwards (0.69 ± 0.03 mg L^{-1}) might have been supplemented by pre-filtration and sampling from the experimental bottles. Although we did not control for this potential artefact, the same protocol was followed for the FN and FD experiments. Therefore, the consistently higher values of DOM consumption, prokaryotic cell size, growth rates and efficiency in the Day compared with the Night incubation strongly support that the presence of fish indeed had a major impact on the microbial community.

Surface specific growth rate in the Day experiment was nevertheless notably higher than the 0.08 d^{-1} measured in a previous study carried out in November 2015 at the same location (Calleja et al. 2018). The discrepancy cannot be explained by total DOC or chlorophyll *a* concentrations, but could instead be related to the availability of labile DOM compounds since C4 concentrations were 61% higher in March than in November (M. L. Calleja, pers. comm.). At a shallower, nearby site characterized by higher total and labile DOC concentrations, specific growth rates were still considerably higher, ranging from 0.79 to 1.75 d^{-1} (Silva et al.).

The daily rates of apparent DOC production and consumption based on changes in in situ concentration were virtually the same within each of the two layers compared, indicating no net accumulation. This is the expected result in oligotrophic regions at the short time scale of one day (Johnson et al. 1981, Wright 1984). However, these rates were still ca. 50% higher in the mesopelagic zone resulting in apparent turnover of labile DOC of 23.6% d^{-1} in the mesopelagic compared with 14.7% d^{-1} at the surface, if we consider the measured diel variability and maximum concentrations in each layer. This finding conflicts with the contention that DOM is largely of refractory nature within the mesopelagic waters of the global ocean (Jiao

et al. 2010). The role of vertically migrating animals, zooplankton and fishes, as vectors of organic matter to deep layers complementary to the biological pump (Herndl and Reinthaler 2013) has been recently recognized (Bianchi et al. 2013, Bianchi et al. 2013, Isla et al. 2015)). In this regard, work at the study site has suggested DVM fishes as a transport mechanism supplying labile DOM that does not accumulate but fuels heterotrohic bacterial activity in mesopelagic waters (Calleja et al. 2018). Here we tested this hypothesis by further examining the fluorescence properties of DOM and its transformation by heterotrophic prokaryotes in experimental incubations with and without the fishes present. FDOM are useful tracers for biogeochemical processes in the dark ocean (Catalá et al. 2015, Nelson and Siegel 2013). Fluorescence intensity of the two aminoacid-like fluorophores C3 and C4 decreased with depth (data not shown), indicating that these fluorophores were mainly produced autochthonously in surface waters. Both phytoplankton and bacteria are sources of tryptophan and tyrosine (Determann et al. 1998), while Urban-Rich et al. (Urban-Rich et al. 2006) have reported that grazing and excretion by zooplankton can also release material with amino acid-like fluorescence signals. Our results strongly suggest that DVM fishes can also provide C4 in the mesopelagic realm.

Contrary to the epipelagic zone, very few studies on the diel variability of DOM-heterotrophic prokaryotes interactions are available for deep waters (Carlucci et al. 1986, García et al. 2018). Gasol et al. (Gasol et al. 2009) suggested that mesopelagic prokaryotes in the subtropical NE Atlantic were as active as in the epipelagic. We demonstrate here not only that heterotrophic prokaryotes specific growth rates at 550 m were of the same order of magnitude than in surface waters, clearly challenging the most accepted view (Arístegui et al. 2009, Baltar et al. 2010), but that those rates were almost double at noon conditions, when the mesopelagic fishes were present, than at midnight, when the entire population was closer to the surface (Klevjer et al. 2012). From **Fig. 1** it is clear that the fishes were absent at midnight in the entire mesopelagic zone but their presence at 550 m had been established for ca. 4 h when the noon sampling took place. Specific growth rates were nevertheless lower than in the previous study (0.24 d^{-1}, (Calleja et al. 2018)). Although seasonality of C4 in the deep scattering layer was less marked than at the surface, November 2015 was characterized by 82% higher C4

concentrations than in March 2016 (M. Calleja, pers. comm.). Altogether, these results point out to a major role of protein-like substances in determining the specific growth rates of heterotrophic prokaryotes throughout the water column, as recently found for nearby shallow waters in a seasonal study (Silva et al.). C4 fluctuated widely in the 24 h monitoring at 550 m depth (**Table S1**) and was also actively consumed in all our incubations, thus revealing a clearly labile nature. C4 was consumed faster in the Fish experiments, at 42.1% and 25.8% d^{-1} in FD and FN, respectively (**Fig. 4, Table S1**), than in the Surface ones (ca. 13% d^{-1} in both SD and SN). A similar relative consumption of protein-like FDOM (12% d^{-1}), mostly occurring during the first 5 days, was measured by (Yamashita and Tanoue 2004) in experiments conducted with marine surface waters. Our explanation is that fishes released DOM directly or it leaked from particles associated to the fish presence (e.g. fecal pellets). That DOM could have been delivered by sinking particles (Smith et al. 1992) not related to vertical migration would not explain the difference between the FD and FN experiments.

Cell size has been used as an indicator of the activity of heterotrophic prokaryotes (Gasol et al. 1995). While in the Surface experiment growing HP cells were only slightly larger than at time 0 (11% larger size for both the SD and SN experiments), the cell size increase in the Fish experiment was dramatic, especially in the Day incubations (118% vs. 68% larger, **Fig. S2**). The contribution of bigger cells to the observed increase in HP biomass is not at all minor: had we used, as in many studies, a fixed cellular carbon content of 4 fg C $cell^{-1}$ (corresponding to the initial mean cell size of 0.027 μm^3 for the two depths and periods, **Fig. 2C**), maximum HP biomass in **Table 1** would have become 2.10 (SD), 2.32, (SN), 0.43 (FD) and 0.39 (FN) $\mu g\ C\ L^{-1}$, i.e. between 42 and 54% lower than the actual values for the mesopelagic prokaryotes. We conclude that the presence of fishes in the mesopelagic zone resulted in significantly higher growth rates of markedly larger cells, exacerbating the changes in biomass relative to those in abundance. The maximum biomass of heterotrophic prokaryotes that could be sustained by extant DOM concentrations was significantly higher than the initial value in both Fish experiments (**Table 1**). Altogether, these results point out to substantial inputs of labile DOM during daytime at the mesopelagic fish layer that are rapidly mobilized by large bacterial taxa. The archaea *Nitrosopulimus maritimus,* which makes up much of the heterotrophic

449 prokaryoplankton biomass at these depths (Ngugi et al. 2012), were apparently not able to
450 respond to these DOM hotspots, since their contribution to total numbers at the end of a
451 similar incubation dropped from 50% to 3% (Calleja et al. 2018). The typical size of
452 Chrenoarcheota is small (Konneke et al. 2005), so it is unlikely that they were the dominant
453 groups growing in our Fish incubations after 2 days (**Fig. S2C, D**). Besides excreting ammonium
454 that boosts anammox by Chrenarcheota (Bianchi et al. 2014), mesopelagic fishes thus seem
455 capable to fuel the metabolism of large, copiotrophic bacteria.
456 Prokaryotic growth efficiencies are typically low in open ocean, oligotrophic
457 environments (del Giorgio and Cole 1998, Reinthaler et al. 2006). The recently reported low
458 PGE values at this Red Sea site (1.6-3.4%, (Calleja et al. 2018) are confirmed by this new study,
459 while higher values(2.5-12.8%) were recorded in a shallow, richer bay located a few km south
460 (Silva et al.). Few studies have estimated the vertical variability in PGE values, but those that
461 have usually depict lower values with depth (Lemée et al. 2002, Reinthaler et al. 2006), related
462 to the increased presence of refractory DOM compounds (Jiao et al. 2010) or to the higher
463 dilution of the labile ones (Arrieta et al. 2015). Notably, the estimated growth efficiency of
464 heterotrophic prokaryotes in our Day experiments was exactly the same in Surface and Fish
465 water (4.2%), which can only be explained by the existence of labile DOC of similar quality
466 within both layers. PGE in the mesopelagic fish layer was significantly higher than at shallower
467 depths in the experiment conducted at noon in November 2015 (Calleja et al. 2018). However,
468 when averaging our new two estimates, the mean PGE value at 550 m (3.6%) was still 22%
469 higher than at the surface, strongly supporting the presence of high quality DOM hotspots
470 (Calleja et al. 2018) in the deep scattering layer.
471 In conclusion, this study confirms that the Red Sea mesopelagic zone is not a
472 permanently impoverished environment but subject to daily inputs of labile DOM compounds
473 similarly to the epipelagic layers. This novel process driven by mesopelagic fishes, which
474 complements other recently discovered sources of deep organic carbon (Boeuf et al. 2019,
475 Dall'Olmo et al. 2016, Giering et al. 2014, Herndl and Reinthaler 2013) seems to have been
476 overlooked due to the tight coupling between the components of microbial food webs
477 (Pernthaler 2005). If vertically migrating fishes are able to fuel an active and distinct community

(T. Huete-Stauffer et al., in prep.) of heterotrophic prokaryotes in the mesopelagic layer of the Red Sea, we might expect this fast DOM flux to be widespread. The mesopelagic Red Sea has an unusually high temperature, therefore the effect of colder conditions on fish DOM-microbial interactions remain to be explored. The implications for global biogeochemical cycling would also vary depending on the actual biomass of mesopelagic fishes and the fraction performing DVM (Klevjer et al. 2016), yet its impact may increase as deep waters warm up (Luna et al. 2012). That these small fishes seem able to sustain the microbial communities inhabiting the twilight zone also may help reconcile current discrepancies between carbon pools and fluxes in the global ocean.

ACKNOWLEDGMENTS

We are greatly indebted to the crew of RV Thuwal and the rest of the personnel from the Coastal and Marine Resources (CMOR) Core Lab at KAUST for their assistance during field work. Besides participating in the sample collection M. Viegas helped us with the rest of the work in the Red Sea Research Center (RSRC) lab. We are also grateful to past and current members of the Microbial Oceanography and Biogeochemistry lab at the RSRC.

X.A.G.M. conceived the research, led the experiment design, data analysis and wrote the paper. F.C.G. modeled in situ growth rates. A.R. performed the acoustic research. L.S. and N. A-O. analyzed the heterotrophic prokaryotes. X.I. contributed to the interpretation of results. M.L.C. was responsible for DOC and FDOM measurements, contributed to experimental design and data analysis. F.C.G., A.R., X.I. and M.L.C. also contributed to writing.

500 **REFERENCES**
501
502 Al-Mutairi, H. and Landry, M. R. 2001. Active export of carbon and nitrogen at Station ALOHA by
503 diel migrant zooplankton. - Deep-Sea Res Pt Ii 48: 2083-2103.
504 Alongi, D. M. and Mukhopadhyay, S. K. 2015. Contribution of mangroves to coastal carbon
505 cycling in low latitude seas. - Agr Forest Meteorol 213: 266-272.
506 Arístegui, J., et al. 2009. Microbial oceanography of the dark ocean's pelagic realm. - Limnol
507 Oceanogr 54: 1501-1529.
508 Arrieta, J. M., et al. 2015. Dilution limits dissolved organic carbon utilization in the deep ocean. -
509 Science 348: 331-333.
510 Baines, S. B. and Pace, M. L. 1991. The production of dissolved organic matter by phytoplankton
511 and its importance to bacteria: Patterns across marine and freshwater systems. - Limnol.
512 Oceanogr. 36 (6): 1078-1090.
513 Baltar, F., et al. 2010. Prokaryotic carbon utilization in the dark ocean: growth efficiency,
514 leucine-to-carbon conversion factors, and their relation. - Aquat Microb Ecol 60: 227-232.
515 Bao, H. Y., et al. 2018. Molecular composition and origin of water-soluble organic matter in
516 marine aerosols in the Pacific off China. - Atmos Environ 191: 27-35.
517 Béjà, O., et al. 2000. Bacterial rhodopsin: evidence for a new type of phototrophy in the sea. -
518 Science 289: 1902-1906.
519 Bianchi, D., et al. 2014. Enhancement of anammox by the excretion of diel vertical migrators. - P
520 Natl Acad Sci USA 111: 15653-15658.
521 Bianchi, D., et al. 2013. Intensification of open-ocean oxygen depletion by vertically migrating
522 animals. - Nat Geosci 6: 545-548.
523 Bianchi, D., et al. 2013. Diel vertical migration: Ecological controls and impacts on the biological
524 pump in a one-dimensional ocean model. - Global Biogeochem Cy 27: 478-491.
525 Boeuf, D., et al. 2019. Biological composition and microbial dynamics of sinking particulate
526 organic matter at abyssal depths in the oligotrophic open ocean. - P Natl Acad Sci USA in press.
527 Bouvier, T., et al. 2007. A comparative study of the cytometric characteristics of High and Low
528 nucleic-acid bacterioplankton cells from different aquatic ecosystems. - Environmental
529 Microbiology 9: 2050-2066.
530 Calbet, A., et al. 2015. Heterogeneous distribution of plankton within the mixed layer and its
531 implications for bloom formation in tropical seas. - Sci Rep-Uk 5.
532 Calleja, M. L., et al. 2019. Dissolved organic carbon contribution to oxygen respiration in the
533 central Red Sea. - Sci Rep-Uk 9: 4690.
534 Calleja, M. L., et al. 2018. The Mesopelagic Scattering Layer: A Hotspot for Heterotrophic
535 Prokaryotes in the Red Sea Twilight Zone. - Front Mar Sci 5.
536 Calleja, M. L., et al. 2018. The Mesopelagic Scattering Layer: A Hotspot for Heterotrophic
537 Prokaryotes in the Red Sea Twilight Zone. - Front Mar Sci 5: 259.
538 Calvo-Díaz, A. and Morán, X. A. G. 2006. Seasonal dynamics of picoplankton in shelf waters of
539 the southern Bay of Biscay. - Aquatic Microbial Ecology 42: 159-174.
540 Carlson, C. A., et al. 1994. Anual flux of dissolved organic carbon from the euphotic zone in the
541 northwestern Sargasso Sea. - Nature 371: 405-408.
542 Carlucci, A. F., et al. 1986. Microheterotrophic Utilization of Dissolved Free Amino-Acids in
543 Depth Profiles of Southern-California Borderland Basin Waters. - Oceanol Acta 9: 89-96.

544 Catalá, T. S., et al. 2015. Turnover time of fluorescent dissolved organic matter in the dark
545 global ocean. - Nat Commun 6: 5986.
546 Coble, P. G. 2007. Marine optical biogeochemistry: The chemistry of ocean color. - Chem Rev
547 107: 402-418.
548 Condon, R. H., et al. 2011. Jellyfish blooms result in a major microbial respiratory sink of carbon
549 in marine systems. - P Natl Acad Sci USA 108: 10225-10230.
550 Dall'Olmo, G., et al. 2016. Substantial energy input to the mesopelagic ecosystem from the
551 seasonal mixed-layer pump. - Nat Geosci 9: 820-+.
552 del Giorgio, P. A. and Cole, J. J. 1998. Bacterial growth efficiency in natural aquatic systems. -
553 Ann. Rev. Ecol. Syst. 29: 503-541.
554 Determann, S., et al. 1998. Ultraviolet fluorescence excitation and emission spectroscopy of
555 marine algae and bacteria. - Mar Chem 62: 137-156.
556 Duarte, C. M. and Cebrián, J. 1996. The fate of marine autotrophic production. - Limnol
557 Oceanogr 41: 1758-1766.
558 Follett, C. L., et al. 2014. Hidden cycle of dissolved organic carbon in the deep ocean. - P Natl
559 Acad Sci USA 111: 16706-16711.
560 Fouilland, E. and Mostajir, B. 2010. Revisited phytoplanktonic carbon dependency of
561 heterotrophic bacteria in freshwaters, transitional, coastal and oceanic waters. - FEMS
562 Microbiology Ecology 73: 419-429.
563 García, F. C., et al. 2018. Diel dynamics and coupling of heterotrophic prokaryotes and dissolved
564 organic matter in epipelagic and mesopelagic waters of the central Red Sea. - Environ Microbiol
565 20: 2990-3000.
566 Gasol, J. M., et al. 2009. Mesopelagic prokaryotic bulk and single-cell heterotrophic activity and
567 community composition in the NW Africa-Canary Islands coastal-transition zone. - Prog
568 Oceanogr 83: 189-196.
569 Gasol, J. M., et al. 1995. Active versus inactive bacteria: size-dependence in coastal marine
570 plankton community. - Mar. Ecol. Prog. Ser. 128: 91-97.
571 Gasol, J. M., et al. 1998. Diel variations in bacterial heterotrophic activity and growth in the
572 northwestern Mediterranean Sea. - Mar. Ecol. Prog. Ser. 164: 107-124.
573 Gasol, J. M. and Morán, X. A. G. 2015. Flow cytometric determination of microbial abundances
574 and its use to obtain indices of community structure and relative activity. - In: McGenity, T. J., et
575 al. (eds.), Hydrocarbon and Lipid Microbiology Protocols. Springer, pp. 159-187.
576 Gasol, J. M., et al. 1999. Significance of size and nucleic acid content heterogeneity as measured
577 by flow cytometry in natural planktonic bacteria. - Appl. Environm. Microbiol. 65: 4475-4483.
578 Giering, S. L. C., et al. 2014. Reconciliation of the carbon budget in the ocean's twilight zone. -
579 Nature 507: 480-+.
580 Goldman, J. C. and Dennett, M. R. 2000. Growth of marine bacteria in batch and continuous
581 culture under carbon and nitrogen limitation. - Limnol Oceanogr 45: 789-800.
582 Gundersen, K., et al. 2001. Particulate organic carbon mass distribution at the Bermuda Atlantic
583 Time-series Study (BATS) site. - Deep-Sea Res. II 48: 1697-1718.
584 Henson, S. A., et al. 2012. Global patterns in efficiency of particulate organic carbon export and
585 transfer to the deep ocean. - Global Biogeochem Cy 26.
586 Herndl, G. J. and Reinthaler, T. 2013. Microbial control of the dark end of the biological pump. -
587 Nat Geosci 6: 718-724.

588 Hunter-Cevera, K. R., et al. 2014. Diel size distributions reveal seasonal growth dynamics of a
589 coastal phytoplankter. - P Natl Acad Sci USA 111: 9852-9857.
590 Irigoien, X., et al. 2014. Large mesopelagic fishes biomass and trophic efficiency in the open
591 ocean. - Nat Commun 5.
592 Isla, A., et al. 2015. Zooplankton diel vertical migration and contribution to deep active carbon
593 flux in the NW Mediterranean. - Journal of Marine Systems 143: 86-97.
594 Jiao, N., et al. 2010. Microbial production of recalcitrant dissolved organic matter: long-term
595 carbon storage in the global ocean. - Nat Rev Microbiol 8: 593-599.
596 Johnson, K. M., et al. 1981. Enigmatic marine ecosystem metabolism measured by direct diel
597 Sigma-CO2 and O-2 flux in conjunction with DOC release and uptake. - Mar Biol 65: 49-60.
598 Klevjer, T. A., et al. 2016. Large scale patterns in vertical distribution and behaviour of
599 mesopelagic scattering layers. - Sci Rep-Uk 6.
600 Klevjer, T. A., et al. 2012. Distribution and diel vertical movements of mesopelagic scattering
601 layers in the Red Sea. - Mar Biol 159: 1833-1841.
602 Konneke, M., et al. 2005. Isolation of an autotrophic ammonia-oxidizing marine archaeon. -
603 Nature 437: 543-546.
604 Lekunberri, I., et al. 2010. Effects of a dust deposition event on coastal marine microbial
605 abundance and activity, bacterial community structure and ecosystem function. - J Plankton Res
606 32: 381-396.
607 Lemée, R., et al. 2002. Seasonal variation of bacterial production, respiration and growth
608 efficiency in the open NW Mediterranean Sea. - Aquatic Microbial Ecology 29: 227-237.
609 Luna, G. M., et al. 2012. The dark portion of the Mediterranean Sea is a bioreactor of organic
610 matter cycling. - Global Biogeochem Cy 26.
611 Morán, X. A. G. and Alonso-Sáez, L. 2011. Independence of bacteria on phytoplankton?
612 Insufficient support for Fouilland & Mostajir's (2010) suggested new concept. - Fems
613 Microbiology Ecology 78: 203-205.
614 Morán, X. A. G., et al. 2011. Single-cell physiological structure and growth rates of
615 heterotrophic bacteria in a temperate estuary (Waquoit Bay, Massachusetts). - Limnol
616 Oceanogr 2011: 37-48.
617 Morán, X. A. G., et al. 2001. Dissolved and particulate primary production and bacterial
618 production in offshore Antarctic waters during austral summer: coupled or uncoupled? -
619 Marine Ecology-Progress Series 222: 25-39.
620 Morán, X. A. G., et al. 2017. Temperature regulation of marine heterotrophic prokaryotes
621 increases latitudinally as a breach between bottom-up and top-down controls. - Global Change
622 Biol 23: 3956-3964.
623 Murphy, K. R., et al. 2010. Measurement of Dissolved Organic Matter Fluorescence in Aquatic
624 Environments: An Interlaboratory Comparison. - Environ Sci Technol 44: 9405-9412.
625 Nagata, T. 2000. Production mechanisms of dissolved organic matter. - In: Kirchman, D. L. (ed.)
626 Microbial ecology of the oceans. Wiley-Liss, pp. 121-152.
627 Nelson, N. B. and Siegel, D. A. 2013. The Global Distribution and Dynamics of Chromophoric
628 Dissolved Organic Matter. - Annual Review of Marine Science, Vol 5 5: 447-476.
629 Ngugi, D. K., et al. 2012. Biogeography of pelagic bacterioplankton across an antagonistic
630 temperature-salinity gradient in the Red Sea. - Mol Ecol 21: 388-405.

631 Pernthaler, J. 2005. Predation on prokaryotes in the water column and its ecological
632 implications. - Nat Rev Microbiol 3: 537-546.
633 Pomeroy, L. R., et al. 2007. The Microbial Loop. - Oceanography 20: 28-33.
634 Reinthaler, T., et al. 2006. Prokaryotic respiration and production in the meso- and bathypelagic
635 realm of the eastern and western North Atlantic basin. - Limnology and Oceanography 51:
636 1262-1273.
637 Robinson, C., et al. 2010. Mesopelagic zone ecology and biogeochemistry - a synthesis. - Deep-
638 Sea Res Pt Ii 57: 1504-1518.
639 Røstad, A., et al. 2016. Light comfort zones of mesopelagic acoustic scattering layers in two
640 contrasting optical environments. - Deep-Sea Research Part I-Oceanographic Research Papers
641 113: 1-6.
642 Ruiz-González, C., et al. 2012. Diel changes in bulk and single-cell bacterial heterotrophic
643 activity in winter surface waters of the northwestern Mediterranean Sea. - Limnol Oceanogr 57:
644 29-42.
645 Ruiz-González, C., et al. 2013. Away from darkness: a review on the effects of solar radiation on
646 heterotrophic bacterioplankton activity. - Front Microbiol 4.
647 Schattenhofer, M., et al. 2011. Phylogenetic characterisation of picoplanktonic populations with
648 high and low nucleic acid content in the North Atlantic Ocean. - Systematic and Applied
649 Microbiology 34: 470-475.
650 Silva, L., et al. Low abundances but high growth rates of heterotrophic bacteria in the coastal
651 Red Sea. - Front Microbiol submitted.
652 Smith, D. C., et al. 1992. Intense Hydrolytic Enzyme-Activity on Marine Aggregates and
653 Implications for Rapid Particle Dissolution. - Nature 359: 139-142.
654 Sosik, H. M., et al. 2003. Growth rates of coastal phytoplankton from time-series measurements
655 with a submersible flow cytometer. - Limnol Oceanogr 48: 1756-1765.
656 Stedmon, C. A. and Bro, R. 2008. Characterizing dissolved organic matter fluorescence with
657 parallel factor analysis: a tutorial. - Limnol Oceanogr-Meth 6: 572-579.
658 Urban-Rich, J., et al. 2006. Larvaceans and copepods excrete fluorescent dissolved organic
659 matter (FDOM). - J Exp Mar Biol Ecol 332: 96-105.
660 Vila-Costa, M., et al. 2012. Community analysis of high- and low-nucleic acid-containing bacteria
661 in NW Mediterranean coastal waters using 16S rDNA pyrosequencing. - Environ Microbiol 14:
662 1390-1402.
663 Wright, R. T. 1984. Dynamics of pools of dissolved organic carbon. - In: Hobbie, J. E. and
664 Williams, P. J. l. B. (eds.), Heterotrophic activity in the sea. Plenum Press, pp. 121-155.
665 Yamashita, Y. and Tanoue, E. 2004. In situ production of chromophoric dissolved organic matter
666 in coastal environments. - Geophys Res Lett 31.
667